Phylomitogenomic Analyses Provided Further Evidence for the Resurrection of the Family Pseudoacanthocephalidae (Acanthocephala: Echinorhynchida)

Tian-You Zhao [1,2,†], **Rui-Jia Yang** [1,2,†], **Liang Lü** [1,2], **Si-Si Ru** [1,2], **Matthew Thomas Wayland** [3], **Hui-Xia Chen** [1,2], **Yuan-Hao Li** [1] and **Liang Li** [1,2,*]

1   Hebei Key Laboratory of Animal Physiology, Biochemistry and Molecular Biology, Hebei Collaborative Innovation Center for Eco-Environment, College of Life Sciences, Hebei Normal University, Shijiazhuang 050024, China
2   Ministry of Education Key Laboratory of Molecular and Cellular Biology, Hebei Research Center of the Basic Discipline Cell Biology, Shijiazhuang 050024, China
3   Department of Zoology, University of Cambridge, Cambridge CB2 3EJ, UK
*   Correspondence: liliang745@hebtu.edu.cn
†   These authors contributed equally to this work.

Simple Summary: Acanthocephalans, commonly known as spiny-headed or thorny-headed worms, are a small group of endoparasites with veterinary, medical and economic importance due to their ability to cause disease in domestic animals, wildlife, and humans. In recent decades, great progress has been made using mitochondrial genome data to clarify the phylogenetic relationships of acanthocephalans. However, the current mitochondrial genome database for acanthocephalans remains very limited. Herein, the characterization of the mitochondrial genome of *Pseudoacanthocephalus bufonis* (Shipley, 1903), the first representative of the family Pseudoacanthocephalidae, is reported. Phylogenetic analyses using the amino acid sequences of 12 protein-coding genes supported the validity of the family Pseudoacanthocephalidae and suggested a close affinity between Pseudoacanthocephalidae and Cavisomatidae. Our phylogenetic results also showed that the families Polymorphidae and Centrorhynchidae have a closer relationship than Plagiorhynchidae in the Polymorphida. These findings contribute to revealing the patterns of mitogenomic evolution in this group and represent a substantial step towards reconstructing the classification of the phylum Acanthocephala.

Abstract: The phylum Acanthocephala is an important monophyletic group of parasites, with adults parasitic in the digestive tracts of all major vertebrate groups. Acanthocephalans are of veterinary, medical, and economic importance due to their ability to cause disease in domestic animals, wildlife, and humans. However, the current genetic data for acanthocephalans are sparse, both in terms of the proportion of taxa surveyed and the number of genes sequenced. Consequently, the basic molecular phylogenetic framework for the phylum is still incomplete. In the present study, we reported the first complete mitochondrial genome from a representative of the family Pseudoacanthocephalidae Petrochenko, 1956. The mitogenome of *Pseudoacanthocephalus bufonis* (Shipley, 1903) is 14,056 bp in length, contains 36 genes (12 protein-coding genes (PCGs) (lacking *atp8*), 22 tRNA genes, and 2 rRNA genes (*rrnL* and *rrnS*)) and two non-coding regions (*NCR1* and *NCR2*), and displayed the highest GC-skew in the order Echinorhynchida. Phylogenetic results of maximum likelihood (ML) and Bayesian inference (BI) using the amino acid sequences of 12 protein-coding genes in different models provided further evidence for the resurrection of the family Pseudoacanthocephalidae and also supported that the order Echinorhynchida is paraphyletic. A monophyletic clade comprising *P. bufonis* and *Cavisoma magnum* suggests a close affinity between Pseudoacanthocephalidae and Cavisomatidae. Our phylogenetic analyses also showed that Polymorphidae has a closer relationship with Centrorhynchidae than Plagiorhynchidae in the monophyletic order Polymorphida.

Keywords: Acanthocephala; Pseudoacanthocephalidae; *Pseudoacanthocephalus*; mitochondrial genome; phylogeny

1. Introduction

Acanthocephala is an important group of obligate endoparasites, with more than 1300 species parasitizing the digestive tracts of all major lineages of vertebrates and their larvae developing in arthropods [1–4]. According to the current classifications based on a combination of morphological and ecological traits, the phylum is divided into three classes, Archiacanthocephala, Eoacanthocephala, and Palaeacanthocephala, which include 10 orders, 26 families, and over 160 genera [1,5–7].

Some previous studies have made efforts to establish a basic molecular phylogenetic framework for Acanthocephala using various nuclear sequence data and mitochondrial genes [8–17]. Recently, mitochondrial genomic data were used to infer the phylogenetic relationships of the higher taxa in Acanthocephala [15,18–25]. However, to date, mitochondrial genome data are available for only 23 species of acanthocephalans, representing 13 families belonging to 6 orders. Several acanthocephalan families and orders were not represented in the above-mentioned phylogenetic studies, due to the paucity and inaccessibility of suitable material or genetic data for these groups.

Echinorhynchida is the largest order in the phylum Acanthocephala, containing more than 470 nominal species, which mainly parasitize teleost fishes but also occur in amphibians and reptiles [1,5,26,27]. Amin (2013) listed 11 families in the Echinorhynchida, including Arhythmacanthidae, Cavisomatidae, Echinorhynchidae, Fessisentidae, Heteracanthocephalidae, Illiosentidae, Isthmosacanthidae, Pomphorhynchidae, Rhadinorhynchidae, Transvenidae, and Sauracanthorhynchidae. Later, two new families, namely Gymnorhadinorhynchidae and Spinulacorpidae, were erected [6,28]. Additionally, two families, Paracanthocephalidae and Pseudoacanthocephalidae, were resurrected [16]. However, the phylogenetic relationships of these families are still uncertain. Additionally, the non-monophyly of Echinorhynchida was also revealed by some previous phylogenetic studies [8–14,17,18,29,30].

In order to further test the monophyly of the orders Echinorhynchida and Polymorphida, assess the validity of the recently resurrected family Pseudoacanthocephalidae, and clarify the evolutionary relationships of the Pseudoacanthocephalidae and the other families in Palaeacanthocephala using mitogenome data, the complete mitochondrial genome of *Pseudoacanthocephalus bufonis*, the first mitogenome from the Pseudoacanthocephalidae, was sequenced and annotated for the first time. Moreover, phylogenetic analyses of the protein-coding genes of all available acanthocephalan mitogenomes were performed using maximum likelihood (ML) and Bayesian inference (BI) in different models.

2. Materials and Methods

2.1. Parasite Collection and Species Identification

A total of 14 spot-legged tree frogs, *Polypedates megacephalus* Hallowell (Anura: Rhacophoridae), were caught by hand at night in the Diaoluo Mountains, Hainan Island, China, and euthanized by injection of an overdose of pentobarbitone sodium solution. The acanthocephalan specimens were collected from the intestine of the host. For light microscopical studies, acanthocephalans were cleared in glycerine. Photomicrographs were recorded using a Nikon® digital camera coupled to a Nikon® optical microscopy (Nikon ECLIPSE Ni-U, Nikon Corporation, Tokyo, Japan). The specimens were identified as *P. bufonis* based on morphological features reported in previous studies [31–36]. The terminology is according to the previous study [37]. Voucher specimens were deposited in the College of Life Sciences, Hebei Normal University, Hebei Province, Shijiazhuang, China (HBNU-A-2022A001L).

2.2. Molecular Procedures

For molecular analysis, the genomic DNA was extracted using a modified CTAB (pH 8.0)-based DNA extraction protocol as described in Zhao et al. [38]. The genomic DNA library was constructed, and a total of 20 GB of clean data were generated using the

pair-end 150 sequencing method on the Illumina NovaSeq 6000 platform by Novogene (Tianjin, China).

The complete mitochondrial genome was assembled using GetOrganelle v1.7.2a [39]. Protein coding genes (PCGs), rRNAs, and tRNAs were annotated using the MitoS web server (http://mitos2.bioinf.uni-leipzig.de/index.py, accessed on 20 January 2022) and MitoZ v2.4 [40]. The open reading frame (ORF) of each PCG was confirmed manually by the web version of ORF finder (https://www.ncbi.nlm.nih.gov/orffinder/, accessed on 10 March 2022). The "lost" tRNA genes ignored by both MitoS and MitoZ were identified using BLAST based on a database of the existing tRNA sequences of Acanthocephala. The secondary structures of tRNAs were predicted by the ViennaRNA module [41], building on MitoS2 [42] and RNAstructure v6.3 [43], followed by a manual correction. MitoZ v2.4 was used to visualize and depict gene element features [40]. The base composition, amino acid usage, and relative synonymous codon usage (RSCU) were calculated by a Python script, which refers to codon adaptation index (CAI) [44]. The total length of the base composition included ambiguous bases. The base skew analysis was used to describe the base composition of nucleotide sequences. The relative values were calculated using the formulas: $ATskew = \frac{A-T}{A+T}$ and $GCskew = \frac{G-C}{G+C}$. The complete mitochondrial genome sequence of *P. bufonis* obtained herein was deposited in the GenBank database (http://www.ncbi.nlm.nih.gov, accessed on 5 October 2022).

2.3. Phylogenetic Analyses

Phylogenetic analyses were performed based on concatenated amino acid sequences of 12 PCGs using maximum likelihood (ML) and Bayesian inference (BI). *Gnathostomula armata* and *G. paradoxa* (Gnathostomulida) were chosen as the out-group. The in-group included 7 species of rotifers and 24 species of acanthocephalans. Detailed information on representatives included in the present phylogeny was provided in Table 1. The phylogenetic trees were re-rooted on Gnathostomulida. Genes were aligned separately using MAFFT v7.313 under the iterative refinement method of E-INS-I [45]. Ambiguous sites and poorly aligned positions were pruned using BMGE v1.12 (m = BLOSUM90, h = 0.5) [46]. The aligned and pruned sequences were concatenated into a matrix by PhyloSuite v1.2.2 [47]. The pruned alignments were then concatenated into the "AA" matrix with the amino acid sequences of PCGs (2087 sites). Bayesian inference (BI) was implemented under the CAT + GTR + G4 model, using PhyloBayes-MPI 1.8 [45,48–51]. Two independent Markov Chain Monte Carlo (MCMC) runs of 8000 generations each were executed. A consensus tree was simultaneously built by pooling the remaining MCMC trees from both runs. Convergence was evaluated with the "bpcomp" and "tracecomp" procedures in the PhyloBayes package with a burn-in of the first 1000 generations. The maximum discrepancy in the convergence result is 0.017. The maximum likelihood (ML) inference was conducted in IQTREE v2.1.2 [52]. Substitution models were compared and selected according to the Bayesian Information Criterion (BIC) by using ModelFinder [53]. Additionally, a profile mixture model (C60) was used based on the best-fit substitution model of the NP datasets of amino acid datasets [54]. An edge-unlinked model was specified for both the full partition and the merged partition schemes. The best run is selected from the four independent runs based on log-likelihood. A total of 1000 Ultrafast bootstraps were used to evaluate the nodal support of the ML tree [55], and to estimate the consensus tree. For the "AA" matrix, three partition schemes were applied for ML (Table 2): (1) no partition (NP); (2) full partition (FP) that provides the best-fitting model for each individual gene; and (3) merged partition (MP) that implements a greedy strategy starting with the full partition model and subsequently merging pairs of genes until the model fit does not improve any further. The phylogenetic-terrace aware (PTA) data structure was used to facilitate the efficient analysis of the "AA" matrix under each partition model [56]. We selected the best final maximum likelihood and consensus trees according to the Akaike Information Criterion (AIC). Phylogenetic analyses ranked nodes with posterior probabilities (PP) and bootstrap support values (BS) = 1/100 as fully supported, 0.98–0.99/95–99 as strongly

supported, 0.95–0.97/90–94 as generally supported, and <90/0.95 as weakly supported. The phylogenetic trees were visualized in iTOL v6.1.1 [57].

Table 1. Detailed information on representatives included in the present phylogeny.

Phylum/Class	Order	Family	Species	Accession	Length	AT%	References
Outgroup							
Gnathostomulida	Bursovaginoidea	Gnathostomulidae	*Gnathostomula armata*	NC_026983	14,030	80.2	[55]
			Gnathostomula paradoxa	NC_026984	14,197	71.8	[55]
Ingroup							
Rotifera	Bdelloidea	Philodinidae	*Rotaria rotatoria*	NC_013568	15,319	73.2	[58]
			Philodina citrina	FR856884	14,003	77.7	[20]
	Monogononta	Brachionidae	*Brachionus calyciflorus*	KX822781	27,683	68.7	[59]
			Brachionus plicatilis	NC_010484	12,672	62.9	[60]
			Brachionus rubens	MN256532	13,795	67.2	[61]
		Proalidae	*Proales similis*	MN970216	16,819	67.2	[62]
	Seisonidea	Seisonidae	*Seison* sp.	KP742964	15,120	70.0	[63]
Acanthocephala							
Archiacanthocephala	Oligacanthorhynchida	Oligacanthorhynchidae	*Macracanthorhynchus hirudinaceus*	NC_019808	14,282	65.2	[20]
			Oncicola luehei	NC_016754	14,281	60.2	[15]
Eoacanthocephala	Gyracanthocephala	Quadrigyridae	*Pallisentis celatus*	NC_022921	13,855	61.5	[64]
			Acanthogyrus bilaspurensis	MT476589	13,360	59.3	unpublished
	Neoechinorhynchida	Neoechinorhynchidae	*Neoechinorhynchus violentum*	KC415004	13,393	59.4	[65]
		Tenuisentidae	*Paratenuisentis ambiguus*	NC_019807	13,574	66.9	[20]
Palaeacanthocephala	Echinorhynchida	Cavisomidae	*Cavisoma magnum*	MN562586	13,594	63.0	[24]
		Echinorhynchidae	*Echinorhynchus truttae*	NC_019805	13,659	63.1	[20]
		Pseudoacanthocephalidae	*Pseudoacanthocephalus bufonis*	MZ958236	14,056	58.4	present study
		Illiosentidae	*Brentisentis yangtzensis*	MK651258	13,864	68.3	[66]
		Pomphorhynchidae	*Pomphorhynchus bulbocolli*	JQ824371	13,915	59.9	unpublished
			Pomphorhynchus laevis	JQ809446	13,889	57.1	unpublished
			Pomphorhynchus rocci	JQ824373	13,845	60.7	unpublished
			Pomphorhynchus tereticollis	JQ809451	13,965	56.9	unpublished
		Rhadinorhynchidae	*Leptorhynchoides thecatus*	NC_006892	13,888	71.4	[67]
	Polymorphida	Centrorhynchidae	*Centrorhynchus clitorideus*	MT113355	15,884	55.5	[68]
			Centrorhynchus milvus	MK922344	14,314	54.5	[22]
			Centrorhynchus aluconis	KT592357	15144	54.5	[19]
			Sphaerirostris lanceoides	MT476588	13,478	58.0	[25]
			Sphaerirostris picae	MK471355	15,170	58.1	[23]
		Polymorphidae	*Polymorphus minutus*	MN646175	14,149	64.4	[69]
			Southwellina hispida	NC_026516	14,742	63.9	[18]
		Plagiorhynchidae	*Plagiorhynchus transversus*	NC_029767	15,477	61.1	[19]
Polyacanthocephala	Polyacanthorhynchida	Polyacanthorhynchidae	*Polyacanthorhynchus caballeroi*	NC_029766	13,956	56.3	[19]

3. Results and Discussion

3.1. Morphology of Pseudoacanthocephalus bufonis (Figure 1, Table 3)

Trunks are medium-sized, smooth, and cylindrical. Females are much larger than males. Proboscis is nearly cylindrical, armed with 16–20 longitudinal rows of 3–5 rooted hooks each. Proboscis receptacle is double-walled with the cerebral ganglion at the posterior of the proboscis receptacle. The neck is short. Lemnisci are more or less equal, slightly longer or shorter than the proboscis receptacle. Morphometric data of the present specimens

and morphometric comparisons of *P. bufonis* between our specimens and previous studies are shown in Table 3.

Table 2. Models, partitioning schemes, and model comparisons of the maximum-likelihood analyses. t: number of partitions; k: number of free parameters; ln (Lik): log-likelihood; AIC: Akaike information criterion; ΔAIC: difference from the minimum AIC; BIC: Bayesian information criterion NP: unpartitioned model; FP: edge-unlinked full partition model; MP: merged and edge-unlinked partition model.

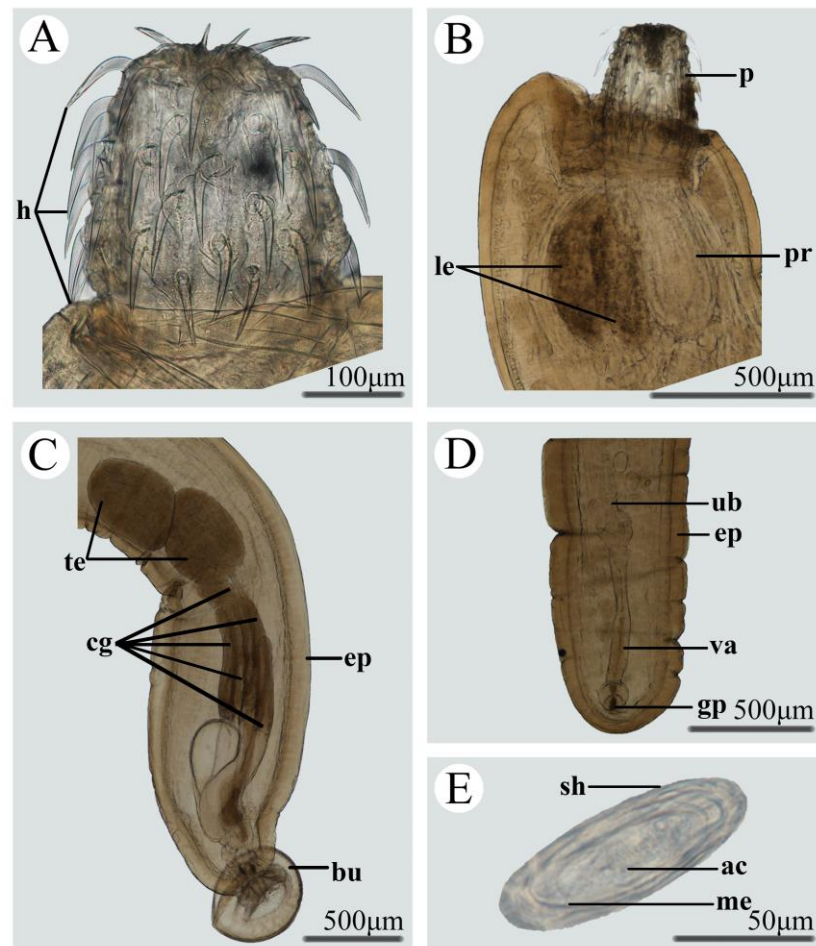| Partition Scheme (t)	Model	Parameters (k)	ln (Lik)	AIC	ΔAIC	BIC
NP (1)	mtZOA + F + R5 + C60	150	−64,770.62	129,841.23		130,683.08
MP (2)	-	112	−64,937.53	130,099.06	257.83	130,727.65
NP (1)	mtZOA + F + R5	90	−65,020.09	130,220.18	378.94	130,725.29
FP (12)	-	287	−64,983.58	130,541.16	699.92	132,151.90

Figure 1. Photomicrographs of *Pseudoacanthocephalus bufonis*. (**A**) Proboscis; (**B**) Presoma of female; (**C**) Metasoma of male; (**D**) Metasoma of female; (**E**) egg. Abbreviations: ac, acanthor; bu, copulatory bursa; cg, cement glands; ep, epidermis; h, hooks; le, lemniscs; me, membrane; p, proboscis; pr, proboscis receptacle; sh, shell of egg, te, testis; ub, uterine bell; va, vagina.

Table 3. Comparative morphometric data for *Pseudoacanthocephalus bufonis* (all measurements are in millimetres).

Host	*Polypedates megacephalus*		*Bufo melanostictus, Rana cancrivora, Takydromus sexlineatus*		*Bufo melanostictus*		*Polypedates megacephalus, P. mutus, Fejervarya limnocharis, Limnonectes kuhlii, Philautus odontotarsus, Odorrana versabilis, Rana livida, Amolops* **sp.**	
Locality	**China**		**Indonesia**		**China**		**China**	
Source	**Present study**		**Kennedy (1982) [32]**		**Wang (1989) [33]**		**Bush (2009) [34]**	
Characteristics	**Male**	**Female**	**Male**	**Female**	**Male**	**Female**	**Male**	**Female**
Trunk length	5.43–8.98	10.0–18.0	5.29–9.38	11.2–16.1	6.80–8.00	15.0–20.0	5.70–11.8	15.3–28.0
Trunk width	1.00–1.50	0.98–1.45	0.98–1.51	1.13–2.10	0.88–1.52	1.40–1.60	1.00–2.20	1.10–2.30
Proboscis length	0.31–0.50	0.38–0.53	0.31–0.44	0.33–0.54	0.48–0.52	0.56–0.64	0.41–0.54	0.41–0.54
Proboscis width	0.28–0.31	0.30–0.41	0.17–0.31	0.22–0.33	0.32–0.45	0.32–0.46	0.28–0.36	0.28–0.36
Lemnisci length	0.48–0.95	0.59–1.23	0.74–1.32	1.16–1.70	0.96–1.44	0.72–1.44	0.80–1.42	0.80–1.42
Proboscis receptacle length	0.41–0.71	0.58–0.91	0.65–0.90	0.88–1.10	0.96–1.12	0.88–1.12	0.69–0.95	0.69–0.95
Proboscis receptacle width	0.25–0.30	0.25–0.45	0.19–0.35	0.31–0.53	0.21–0.32	0.24–0.32	0.27–0.35	0.27–0.35
Size of the anterior testis	0.45–0.80 × 0.40–0.62	N/A	0.47–0.79 × 0.31–0.53	N/A	0.56–0.68 × 0.40–0.48	N/A	0.51–0.95 × 0.29–0.58	N/A
Size of the posterior testis	0.45–0.74 × 0.37–0.65	N/A	0.54–0.72 × 0.28–0.50	N/A	0.52–0.72 × 0.48–0.51	N/A	0.51–0.95 × 0.29–0.58	N/A
Cement-gland length	0.76–1.46	N/A	–	N/A	–	N/A	0.77–1.51	N/A
Size of the copulatory bursa	0.40–0.46 × 0.46–0.84	N/A	–	N/A	–	N/A	–	N/A
Uterine bell length	N/A	0.34–0.62	N/A	–	N/A	0.80–0.85	N/A	0.45–0.68
Uterus length	N/A	0.26–0.47	N/A	–	N/A	–	N/A	0.29–0.38
Size of the egg	N/A	0.06–0.09 × 0.02–0.03	N/A	0.08–0.09 × 0.02–0.03	N/A	0.06–0.09 × 0.02–0.03	N/A	0.06–0.07 × 0.02

The morphology and measurements of the present material are more or less identical to the previous descriptions of *P. bufonis* [31–36], including the morphology and size of trunk and proboscis, the number of the longitudinal rows of proboscis hooks and the hooks per longitudinal row, the number and length of testes and cement-glands, and the morphology and size of eggs. However, the lengths of the proboscis receptacle and lemnisci are slightly ser than those of the previous studies. Additionally, we also sequenced the ITS region (OQ550505, OQ550506) of our specimens. Pairwise comparison of the ITS sequences of our specimens with the available ITS data (KC491878–KC491883) of *P. bufonis* reported in the previous study [70], displayed only 0.17% nucleotide divergence. Thus, we confirmed our specimens to be *P. bufonis*.

3.2. Gene Content and Organization of the Mitogenome

The complete mitogenome of *P. bufonis* is 14,056 bp in length and includes 36 genes, containing 12 PCGs (*cox1–3*, *nad1–6*, *nad4l*, *cytb*, and *atp6*), 22 tRNA genes, 2 rRNA genes (*rrnS* and *rrnL*), and two non-coding regions (*NCR1* and *NCR2*) (Figure 2, Table 4). The lack of *atp8* in the mitogenome of *P. bufonis* is typical for most of the available mitogenomes of acanthocephalans, except for *Leptorhynchoides thecatus*, which has two putative *atp8* genes [55]. All genes in the mitogenome of *P. bufonis* are encoded on the same strand and in the same direction. Furthermore, the highest GC-skew (0.53) and the second lowest AT-skew (−0.28) of the mitogenome of *P. bufonis* in the order Echinorhynchida show its preference for G and T nucleotides (Figure 3), which was possibly a result of the propensity for low use of A-rich codons in their PCGs (Table 5). A similar situation also occurred in *Polyacanthorhynchus caballeroi* and some species of Polymorphida [19,21,25].
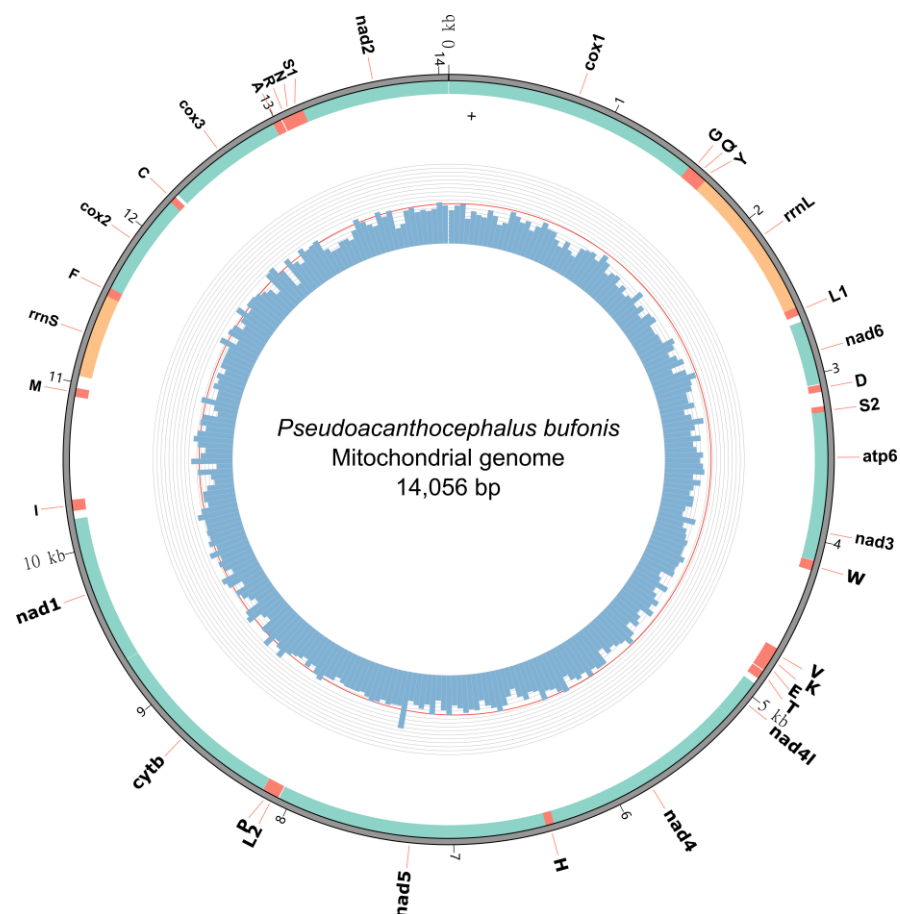

Figure 2. Gene map of the mitochondrial genome of *Pseudoacanthocephalus bufonis*. The outermost circle shows the gene features, sandy brown for rRNAs, salmon for tRNAs, and light sea green for PCGs. The innermost circle shows the GC content calculated in every 50-site window.

Table 4. Annotations and gene organization of *Pseudoacanthocephalus bufonis*. The positive number in the "Gap or overlap" column indicates the length of intergenic sequence, and the negative number indicates the length (absolute number) that adjacent genes overlap (negative sign).

| Gene	Type	Start	End	Length	Start Codon	Stop Codon	Anticodon	Gap or Overlap
cox1	CDS	1	1539	1539	GTG	TAG		−2
trnG	tRNA	1538	1589	52			UCC	−11
trnQ	tRNA	1579	1641	63			UUG	−13
trnY	tRNA	1629	1679	51			GUA	1
rrnL	rRNA	1681	2588	908				0
trnL1	tRNA	2589	2638	50			UAG	0
nad6	CDS	2639	3063	425	GTG	TA		4
trnD	tRNA	3068	3111	44			GUC	85
trnS2	tRNA	3197	3253	57			UGA	−22
atp3	CDS	3232	3771	540	ATA	TAA		−1
nad3	CDS	3771	4118	348	ATG	TAA		1
trnW	tRNA	4120	4179	60			UCA	0
NCR2	Non-coding region	4180	4682	503				0
trnV	tRNA	4683	4742	60			UAC	−14
trnK	tRNA	4729	4793	65			UUU	−11
trnE	tRNA	4783	4833	51			UUC	5
trnT	tRNA	4839	4894	56			UGU	35
nad4l	CDS	4930	5172	243	GTG	TAA		0
nad4	CDS	5173	6397	1225	ATG	T		1
trnH	tRNA	6399	6453	55			GUG	−6
nad5	CDS	6448	8067	1620	GTG	TAG		4
trnL2	tRNA	8072	8133	62			UAA	−23
trnP	tRNA	8111	8173	63			UGG	0
cytb	CDS	8174	9298	1125	TTG	TAA		1
nad1	CDS	9300	10,190	891	ATT	TAA		47
trnI	tRNA	10,238	10,305	68			GAU	0
NCR1	Non-coding region	10,306	10,915	610				0
trnM	tRNA	10,916	10,969	54			CAU	0
rrnS	rRNA	10,970	11,541	572				0
trnF	tRNA	11,542	11,605	64			GAA	8
cox2	CDS	11,614	12,216	603	TTG	TAG		−2
trnC	tRNA	12,215	12,256	42			GCA	19
cox3	CDS	12,276	12,978	703	GTG	T		0
trnA	tRNA	12,979	13,032	54			UGC	5
trnR	tRNA	13,038	13,089	52			UCG	−20
trnN	tRNA	13,070	13,127	58			GUU	−10
trnS1	tRNA	13,118	13,174	57			ACU	−1
nad2	CDS	13,175	14,055	882	GTG	TAA		1
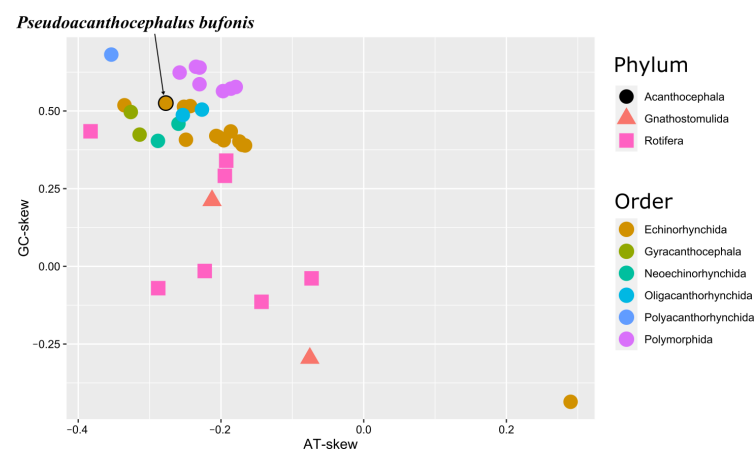
Figure 3. Comparison of genome-wide nucleotide skews among Acanthocephala, Gnathostomulida, and Rotifera. Species of Acanthocephala are coloured according to their taxonomic placement at the Order level.

Table 5. Base composition and skewness of *Pseudoacanthocephalus bufonis*.

Location	A%	T%	C%	G%	AT%	AT-Skew	GC-Skew	Total
Whole mitochondrial genome	34.35	37.31	9.87	31.71	58.42	−0.28	0.53	14,056
Protein coding genes (PCGs)	18.88	38.07	9.27	33.78	56.95	−0.45	2.65	10,144
1st codon	21.58	30.12	9.58	38.72	51.70	−0.18	3.04	3383
2nd codon	13.07	47.97	10.68	28.28	61.05	−0.90	1.65	3381
3rd codon	21.98	36.12	7.54	34.35	58.11	−0.34	3.56	3380
tRNAs	25.20	37.48	10.50	26.82	62.68	−0.20	0.44	1238
rRNAs	28.18	35.54	10.61	25.68	63.72	−0.12	0.42	63.72
rrnS	27.97	37.06	8.74	26.22	65.03	−0.14	0.50	65.03
rrnL	28.30	34.58	11.78	25.33	62.89	−0.10	0.37	62.89
Non-coding region 1	28.36	33.61	19.34	18.69	61.97	−0.08	−0.02	610
Non-coding region 2	26.64	30.22	5.57	37.57	56.86	−0.06	0.74	503

3.3. Protein-Coding Genes and Codon Usage

The length of 12 PCGs is 10,114 bp. 12 PCGs encode 3358 amino acids and include 3358 codons, excluding termination codons. The longest PCG is *nad5* (1620 bp), while the shortest PCG is *nad4l* (243 bp) (Figure 2, Table 4).

The composition and usage of codons in the mitogenome of *P. bufonis* were shown in Figure 4 and Table 6. ATN (i.e., ATA, ATG, and ATT), GTG, and TTG are used as start codons for the 12 PCGs in the mitogenome of *P. bufonis*, whereas TAA, TAG, and incomplete codons of T or TA are used as termination codons, in accordance with those of other acanthocephalans [15,18–25,58–64]. GTG is the most common start codon, being used for six PCGs (*cox1, cox3, nad2, nad4l, nad5,* and *nad6*), followed by ATN for four PCGs (ATA: *atp6*; ATG: *nad3* and *nad4*; ATT: *nad1*). Two genes (*cytb* and *cox2*) were inferred to use TTG as the start codon. Among the 12 PCGs, six genes (*atp6, cytb, nad1, nad2, nad3,* and *nad4l*) are terminated with complete stop codon TAA, while three genes (*cox1, cox2,* and *nad5*) were inferred to terminate with complete stop codon TAG. The incomplete stop codons T and TA are used for *cox3* and *nad4,* and *nad6,* respectively.
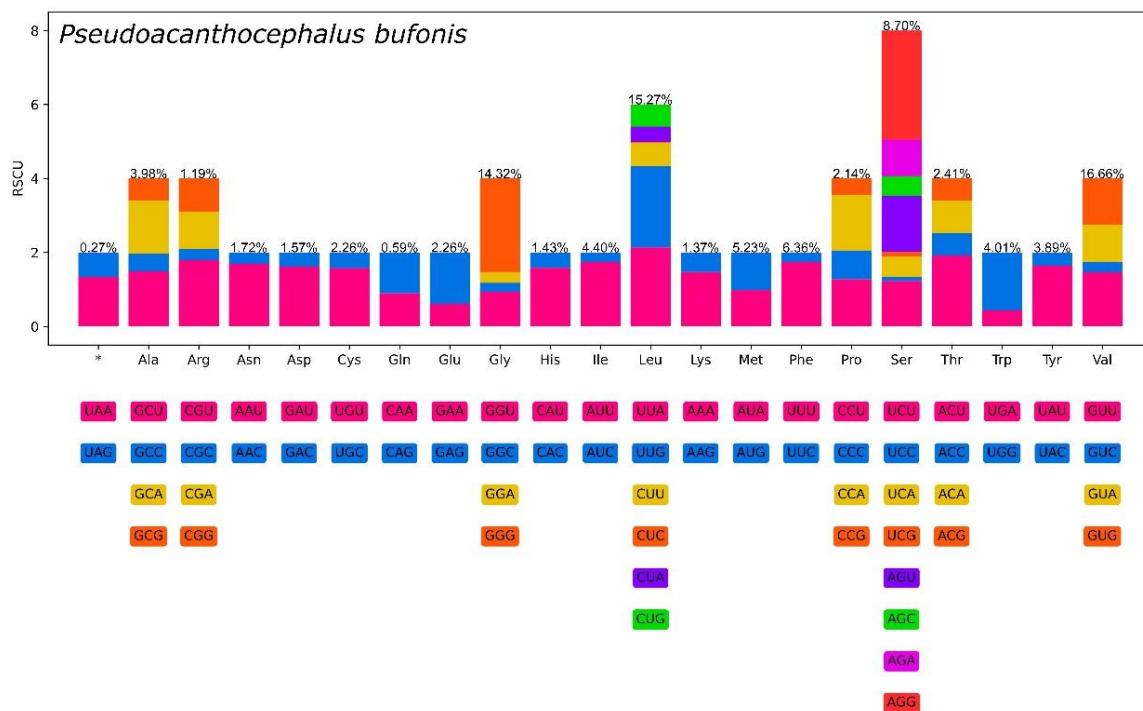

Figure 4. Relative synonymous codon usage (RSCU) of *Pseudoacanthocephalus bufonis*. Codon families (in alphabetical order) are provided below the horizontal axis.

Table 6. Relative synonymous codon usage (RSCU) of *Pseudoacanthocephalus bufonis* (The asterisk represents termination codon).

Codon	aa	No.	%	Codon	aa	No.	%
TAA	*	6	0.18	TTA	Leu	183	5.44
TAG	*	3	0.09	TTG	Leu	188	5.58
GCA	Ala	48	1.43	AAA	Lys	34	1.01
GCC	Ala	16	0.48	AAG	Lys	12	0.36
GCG	Ala	20	0.59	ATA	Met	86	2.55
GCT	Ala	50	1.49	ATG	Met	90	2.67
CGA	Arg	10	0.30	TTC	Phe	28	0.83
CGC	Arg	3	0.09	TTT	Phe	186	5.52
CGG	Arg	9	0.27	CCA	Pro	27	0.80
CGT	Arg	18	0.53	CCC	Pro	14	0.42
AAC	Asn	9	0.27	CCG	Pro	8	0.24
AAT	Asn	49	1.46	CCT	Pro	23	0.68
GAC	Asp	10	0.30	AGA	Ser	36	1.07
GAT	Asp	43	1.28	AGC	Ser	20	0.59
TGC	Cys	16	0.48	AGG	Ser	108	3.21
TGT	Cys	60	1.78	AGT	Ser	55	1.63
CAA	Gln	9	0.27	TCA	Ser	20	0.59
CAG	Gln	11	0.33	TCC	Ser	4	0.12
GAA	Glu	23	0.68	TCG	Ser	5	0.15
GAG	Glu	53	1.57	TCT	Ser	45	1.34
GGA	Gly	36	1.07	ACA	Thr	18	0.53
GGC	Gly	28	0.83	ACC	Thr	12	0.36
GGG	Gly	304	9.03	ACG	Thr	12	0.36
GGT	Gly	114	3.39	ACT	Thr	39	1.16
CAC	His	10	0.30	TGA	Trp	29	0.86
CAT	His	38	1.13	TGG	Trp	106	3.15
ATC	Ile	19	0.56	TAC	Tyr	23	0.68
ATT	Ile	129	3.83	TAT	Tyr	108	3.21
CTA	Leu	35	1.04	GTA	Val	139	4.13
CTC	Leu	2	0.06	GTC	Val	41	1.22
CTG	Leu	51	1.51	GTG	Val	176	5.23
CTT	Leu	55	1.63	GTT	Val	205	6.09

　　　In the PCGs of *P. bufonis*, the codon with the highest RSCU value is AGG (Ser), while the rarest codon is CTC (Leu). Val is the most frequently used amino acid (16.66%) in 12 PCGs of *P. bufonis*. Gln is the least commonly used amino acid (0.59%). The high frequency of Val (encoded by GTN) is associated with the high proportions of G and T in their protein-coding sequences (Figure 4 and Table 6).

3.4. Ribosomal and Transfer RNAs

　　　A total of 22 tRNAs were identified, ranging in length from 42 bp (*trnC*) to 68 bp (*trnI*) (Table 4). The anticodons (Table 4) and secondary structures (Figure 5) of the 22 tRNAs were identified. Of the 22 tRNAs, four (*trnA*, *trnN*, *trnL2*, *trnS1*) have a short dihydrouridine (DHU) arm, six (*trnA*, *trnE*, *trnG*, *trnI*, *trnL1*, *trnY*) lack a TψC (T) arm, and two (*trnD* and *trnC*) have lost both arms (Figure 5). Moreover, the *trnT* has a short amino acid acceptor (AA) arm. The other nine tRNAs were predicted to be folded into typical cloverleaf secondary structures, as found in other acanthocephalans [19,23].

　　　In the mitogenome of *P. bufonis*, two rRNAs, *rrnL*, located between *trnY* and *trnL1*, and *rrnS*, located between *trnM* and *trnP*, were identified. The *rrnL* is 908 bp in length, with 62.86% A + T content, whereas the *rrnS* is 572 bp in length with 64.37% A + T content (Figure 2 and Table 5).
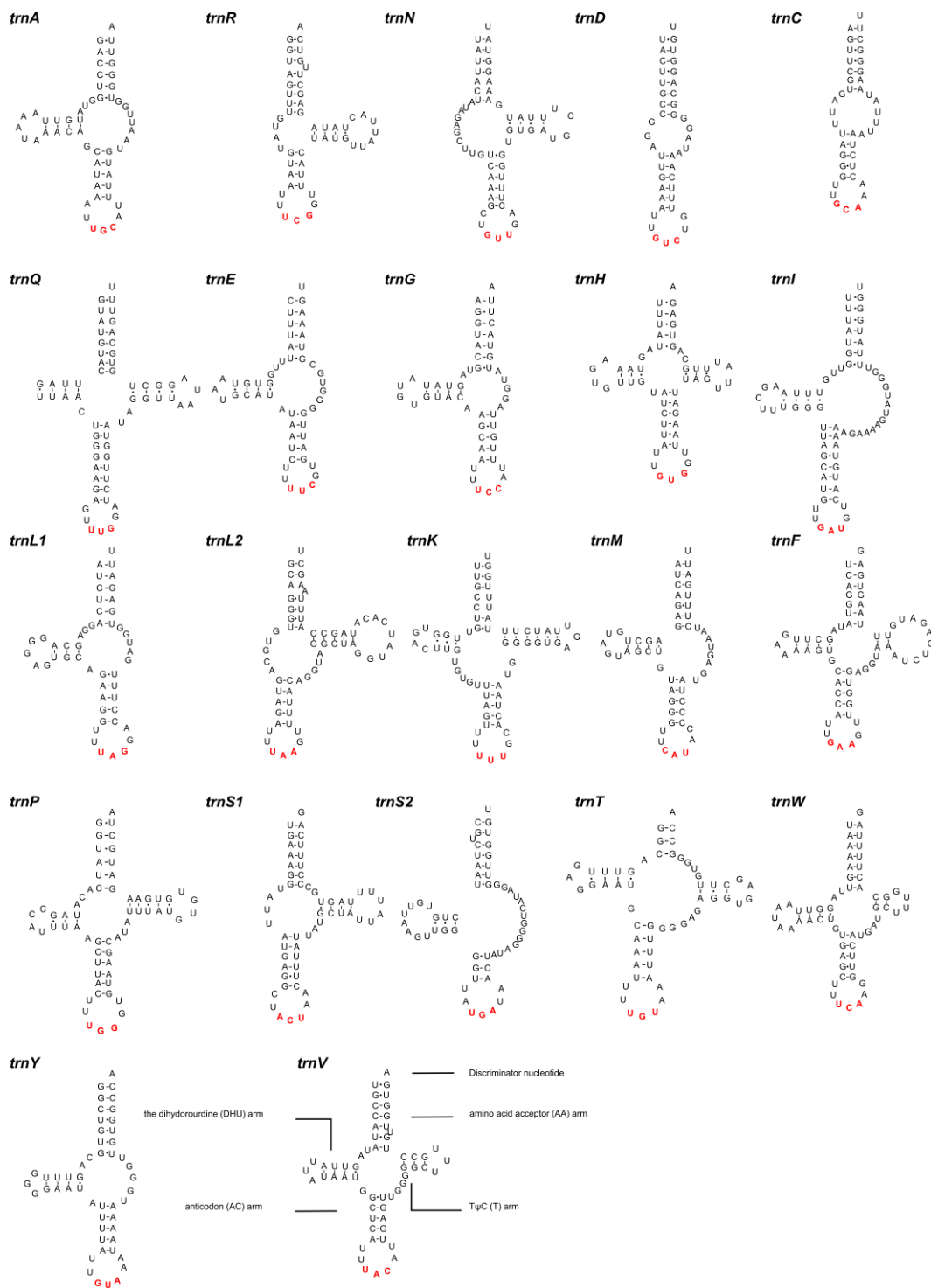
Figure 5. Predicted secondary structures of 22 tRNAs in the mitogenome of *Pseudoacantho-cephalus bufonis* (Watson-Crick bonds indicated by lines, GU bonds indicated by dots, red bases representing anticodons).

3.5. Gene Order

In the mitogenome of *P. bufonis*, gene arrangement of PCGs and rRNAs is in the following order: *cox1, rrnL, nad6, atp6, nad3, nad4l, nad4, nad5, ctyb, nad1, rrnS, cox2, cox3,* and *nad1,* a pattern which appears to be relatively conserved in acanthocephalans [22–25,64]. However, some tRNAs (i.e., *trnS1, trnS2, trnM, trnV, trnK, trnR,* and *trnC*) show more variability in

translocation [21,65]. There are up to three translocations in tRNAs in the mitogenome of acanthocephalans reported so far (i.e., *trnS1*, *trnS2*, and *trnK*) [18,20,22–24,66] (Figure 6). There are two main gene arrangements of *trnS2*: type A (*trnS2*, *atp6*, *nad3*, *trnW*, *trnV*, *trnK*, *trnE*, and *trnT*) and type B (*atp6*, *nad3*, *trnW*, *trnV*, *trnK*, *trnE*, *trnT*, and *trnS2*). The *trnK* has two arrangements: type C (*trnK* and *trnV*) and type D (*trnV* and *trnK*). The gene arrangement of *trnS1* has three order types: type E (*trnS1*, *trnM*, *rrnS*, *trnF*, *cox2*, *trnC*, *cox3*, *trnA*, *trnR*, and *trnN*), type F (*trnM*, *rrnS*, *trnF*, *cox2*, *trnC*, *cox3*, *trnA*, *trnR*, *trnN*, and *trnS1*), and type G (*trnM*, *trnS1*, *rrnS*, *trnF*, *cox2*, *trnC*, *cox3*, *trnA*, *trnR*, and *trnN*) [18,20,22–24,59,66,67]. In the mito-genome of *P. bufonis*, *trnR* is situated between *trnA* and *trnN*, while *trnS2* lays between *trnD* and *atp6* (Figure 6).
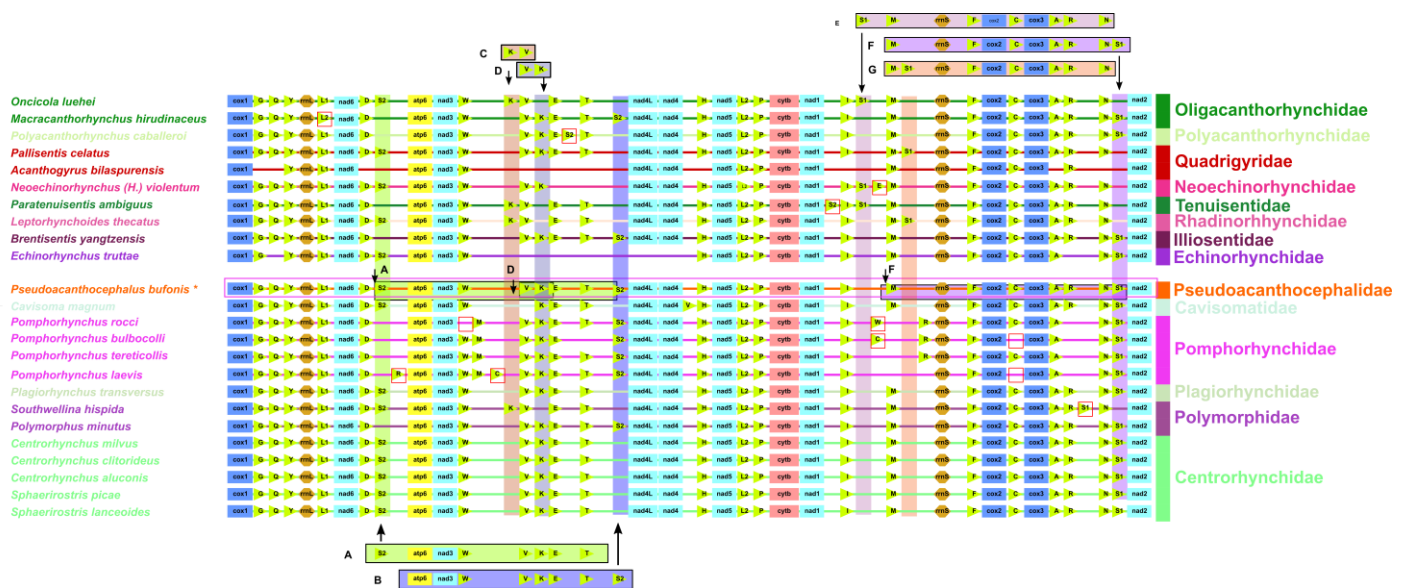
Figure 6. Comparison of the linearized mitochondrial genome arrangement for 24 acanthocephalans species. All genes are transcribed in the same direction, from left to right. The tRNAs are labelled by a single-letter code for the corresponding amino acid. A–B: the position of *trnS2*; C–D: the position of *trnK*; E–G: the position of *trnS1*. Translocations of individual *tRNAs* are marked with red boxes. The shadowed regions highlighted bin pink represent Pomphorhynchidae (*Pseudoacanthocephalus bufonis* indicated by asterisk).

The gene order of *trnS2* in the mitogenome of *P. bufonis* is type A (*trnS2*, atp6, *nad3*, *trnW*, *trnV*, *trnK*, *trnE*, *trnT*). The gene arrangement of *trnK* is of type D (*trnK*, *trnV*). The *trnS1* of *P. bufonis* is of type F (*trnM*, *rrnS*, *trnF*, *cox2*, *trnC*, *cox3*, *trnA*, *trnR*, *trnN*, *trnS1*) (Figure 6).

3.6. Non-Coding Regions

In the mitogenome of *P. bufonis*, there are two non-coding regions (*NCR1* and *NCR2*). *NCR1* is located between *trnI* and *trnM*, is 610 bp in length. *NCR2,* located between *trnW* and *trnV*, is 503 bp. Their A + T contents are 61.97% and 56.86%, respectively (Table 5).

3.7. Molecular Phylogeny

Phylogenetic trees generated from BI and ML methods under different models have similar topologies and indicate that the Acanthocephala are monophyletic, which was widely accepted in previous studies. However, the evolutionary relationships of the Acanthocephala and the three subtaxa of Rotifera (Monogononta, Bdelloidea, and Seisonidea) have been under debate for a long time [19,71–73]. The present phylogenetic results showed that the Acanthocephala is sister to Bdelloidea (*Rotaria rotatoria*, *Philodina citrina*) and rejected the monophyly of Eurotatoria (Monogononta + Bdelloidea), which are identical to

the previous phylogenetic results using EST libraries [72] and mitogenomic data [19], but conflicted with some other phylogenies based on 18S rDNA and transcriptomic data [71,73].

Our phylogeny also supported the division of the phylum Acanthocephala into three large clades (Clade I, Clade II, and Clade III) (Figure 7). Clade I, including *Macracanthorhynchus hirudinaceus* and *Oncicola luehei* (Oligacanthorhynchida: Oligacanthorhynchidae), represents Archiacanthocephala, a monophyletic group located at the base of the phylogenetic trees of Acanthocephala (Figure 7). The present results agree well with some previous phylogenetic studies [8,9,11–13,18,20,22–25,64,66]. The representative of Polyacanthocephala (*Polyacanthorhynchus caballeroi*) nested with species of Eoacanthocephala (*Pallisentis celatus* + *Acanthogyrus bilaspurensis* + *Neoechinorhynchus violentum* + *Paratenuisentis ambiguus*), forming Clade II. The present phylogenetic results challenged the validity of Polyacanthocephala, as have some previous molecular phylogenetic studies [19,22,23,25,64,66].
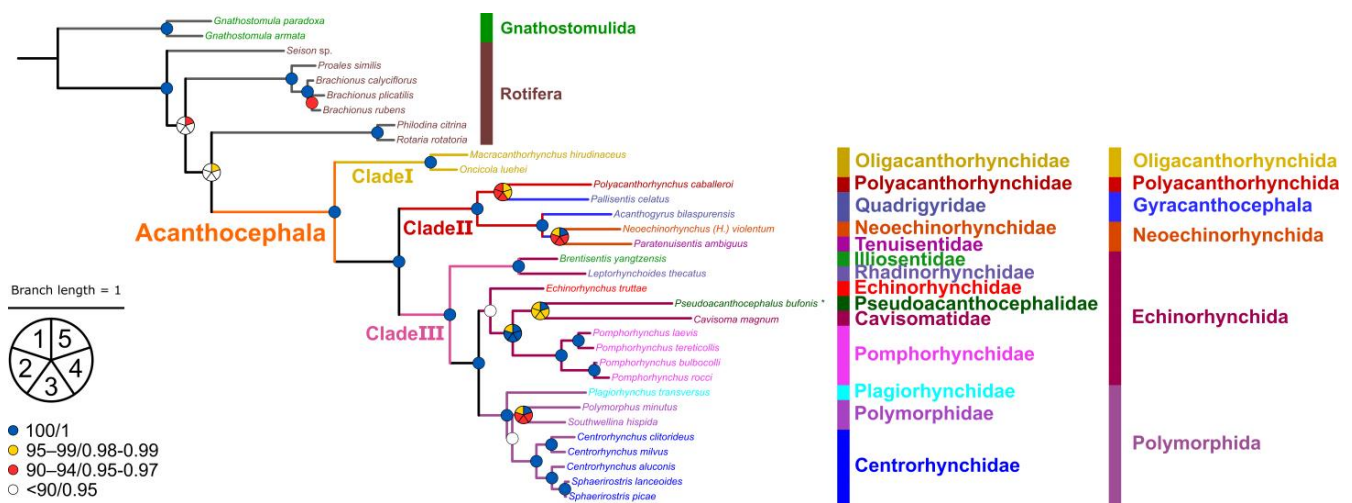

Figure 7. Phylogenetic relationships of Acanthocephala are presented based on the topology of Bayesian inference results. The branch length scale is marked according to the tree of Bayesian inference. The species followed by an asterisk (*) are sequenced in this study. Coloured circles indicate posterior probabilities/bootstrap support. Nodes of the cladogram with 0.95–0.97/90–94 are labelled orange; 0.98–0.99/95–99 by blue; 1/100 by green. Nodes divided into five parts indicate the different supports of five methods: (1) Bootstrap support of ML methods with no partition (NP) scheme under the mtZOA + F + R5 model; (2) with full partition (FP) scheme; (3) with merged partition (MP) scheme; (4): Bootstrap support of ML methods under the mtZOA + F + R5 + C60 model; and (5) Posterior probabilities of Bayesian inference.

The representatives of Palaeacanthocephala formed Clade III. The monophyly of the order Polymorphida, including the representatives of *Plagiorhynchus transversus*, *Polymorphus minutus*, *Southwellina hispida*, *Centrorhynchus clitorideus*, *C. milvus*, *C. aluconis*, *Sphaerirostris lanceoides*, and *S. picae*, is strongly supported in our phylogenetic results. In Polymorphida, the Polymorphidae are more closely related to the Centrorhynchidae than the Plagiorhynchidae, in accordance with other recent mitogenomic phylogenies, but inconsistent with some previous phylogenetic studies based on nuclear and mitochondrial genetic markers [17,68,69,74]. Our phylogenetic results showed that the order Echinorhynchida is paraphyletic, which is consistent with previous molecular phylogenetic studies [12,14,28,30,69]. Furthermore, they supported the resurrection of Pseudoacanthocephalidae [16]. In the present mitogenomic phylogeny, *P. bufonis* clustered together with *Cavisoma magnum*, suggesting an affinity between Pseudoacanthocephalidae and Cavisomatidae. Our results agreed well with some recent phylogenetic studies based on nuclear gene sequences [16,75]. These indicated that the current classification of Echinorhynchida is based on unique combinations of characteristics, not shared derived features [13]. The systematics of Echinorhynchida needs to be revised so that its constituent families, subfamilies,

and genera reflect the underlying lineages. This will require phylogenetic analysis of both nuclear and mitochondrial DNA datasets from representatives of a more diverse range of taxa than are currently available. It is essential to sequence mitogenomes from yet unrepresented taxa for constructing the molecular phylogenetic framework of Acanthocephala and further exploring the unusual patterns of mitogenomic evolution in this group. The complete mitogenome of *P. bufonis* obtained herein represents a valuable building block for future work.

4. Conclusions

In the present study, the complete mitochondrial genome of *P. bufonis*, the first representative of the family Pseudoacanthocephalidae, was characterized. Phylogenetic analyses based on the amino acid sequences of 12 protein-coding genes further confirmed the sister relationship of the Acanthocephala and Bdelloidea and rejected the monophyly of Eurotatoria (Monogononta + Bdelloidea) and Pararotatoria (Seisonidea + Acanthocephala). Our phylogeny also revealed that the order Echinorhynchida and the family Echinorhynchidae are both paraphyletic in the Acanthocephala. The current systematic status of *Pseudoacanthocephalus* in the Echinorhynchidae is challenged. The present phylogenetic results supported the recent resurrection of Pseudoacanthocephalidae and showed a close affinity between Pseudoacanthocephalidae and Cavisomatidae. Phylogenetic analyses also strongly supported the monophyly of the order Polymorphida and indicated that the Polymorphidae and Centrorhynchidae have a closer relationship than the Plagiorhynchidae. The present phylogenetic studies provided a new insight into the evolutionary relationships of higher taxa within Acanthocephala.

Author Contributions: Contributed to the study design and analyze genetic data, T.-Y.Z., R.-J.Y. and L.L. (Liang Li); collected and identified the acanthocephalan specimens, S.-S.R., H.-X.C., Y.-H.L. and L.L. (Liang Li); conducted the phylogenetic analyses, T.-Y.Z., R.-J.Y., L.L. (Liang Lü) and L.L. (Liang Li); wrote and revised the manuscript, T.-Y.Z., R.-J.Y., M.T.W. and L.L. (Liang Li). All authors have read and agreed to the published version of the manuscript.

Institutional Review Board Statement: This study was conducted under the protocols of Hebei Normal University. All applicable national and international guidelines for the protection of animals were followed. All experimental procedures involving animals in this study, including the autopsy, were approved by the Animal Ethics Committee of Hebei Normal University, China (no. 2023LLSC001).

Informed Consent Statement: Not applicable.

Data Availability Statement: The mitogenome sequence of *Pseudoacanthocephalus bufonis* obtained in this study was deposited in the GenBank database. Voucher specimens of *P. bufonis* were deposited in the College of Life Sciences, Hebei Normal University, Hebei Province, under the accession number HBNU-A-2022A001L.

Conflicts of Interest: The authors declare no conflict of interest.

References

1. Amin, O.M. Classification of the Acanthocephala. *Folia. Parasitol.* **2013**, *60*, 273–305. [CrossRef] [PubMed]
2. Yamaguti, S. Acanthocephala. In *Systema Helminthum*; Interscience Publishers John Wiley and Sons: New York, NY, USA, 1963; Volume V, pp. 1–423.
3. Kennedy, C.R. *Ecology of the Acanthocephala*; Cambridge University Press: Cambridge, UK, 2006; ISBN 978-0-521-85008-7.
4. Schmidt, G.D. Development and life cycles. In *Biology of Acanthocephala*; Crompton, D.W.T., Nickol, B.B., Eds.; Cambridge University Press: Cambridge, UK, 1985; pp. 273–286.
5. Amin, O.M. Key to the families and subfamilies of acanthocephala, with the Erection of a new class (Polyacanthocephala) and a new order (Polyacanthorhynchida). *J. Parasitol.* **1987**, *73*, 1216–1219. [CrossRef] [PubMed]
6. Huston, D.C.; Smales, L.R. Proposal of *Spinulacorpus biforme* (Smales, 2014) n. g., n. comb. and the Spinulacorpidae n. fam. to resolve paraphyly of the acanthocephalan family Rhadinorhynchidae Lühe, 1912. *Syst. Parasitol.* **2020**, *97*, 477–490. [CrossRef] [PubMed]

7. Zhang, Z.-Q. Animal biodiversity: An outline of higher-level classification and survey of taxonomic richness. *Zootaxa* **2011**, *3148*, 63–95. [CrossRef]

8. Near, T.J.; Garey, J.R.; Nadler, S.A. Phylogenetic relationships of the Acanthocephala inferred from 18S ribosomal DNA Sequences. *Mol. Phylogenet. Evol.* **1998**, *10*, 287–298. [CrossRef]

9. García-Varela, M.; Pérez-Ponce de León, G.; de la Torre, P.; Cummings, M.P.; Sarma, S.S.S.; Laclette, J.P. Phylogenetic relationships of Acanthocephala based on analysis of 18S ribosomal RNA gene sequences. *J. Mol. Evol.* **2000**, *50*, 532–540. [CrossRef]

10. García-Varela, M.; Cummings, M.P.; Pérez-Ponce de León, G.; Gardner, S.L.; Laclette, J.P. Phylogenetic analysis based on 18S ribosomal RNA gene sequences supports the existence of class Polyacanthocephala (Acanthocephala). *Mol. Phylogenet. Evol.* **2002**, *23*, 288–292. [CrossRef]

11. Near, T.J. Acanthocephalan phylogeny and the evolution of parasitism1. *Integr. Comp. Biol.* **2002**, *42*, 668–677. [CrossRef]

12. Verweyen, L.; Klimpel, S.; Palm, H.W. Molecular phylogeny of the Acanthocephala (class Palaeacanthocephala) with a paraphyletic assemblage of the orders Polymorphida and Echinorhynchida. *PLoS ONE* **2011**, *6*, e28285. [CrossRef]

13. García-Varela, M.; Nadler, S.A. Phylogenetic relationships of Palaeacanthocephala (Acanthocephala) inferred from SSU and LSU rDNA gene sequences. *J. Parasitol.* **2005**, *91*, 1401–1409. [CrossRef]

14. García-Varela, M.; Nadler, S.A. Phylogenetic relationships among Syndermata inferred from nuclear and mitochondrial gene sequences. *Mol. Phylogenet. Evol.* **2006**, *40*, 61–72. [CrossRef]

15. Gazi, M.; Sultana, T.; Min, G.-S.; Park, Y.C.; García-Varela, M.; Nadler, S.A.; Park, J.-K. The complete mitochondrial genome sequence of *Oncicola luehei* (Acanthocephala: Archiacanthocephala) and its phylogenetic position within Syndermata. *Parasitol. Int.* **2012**, *61*, 307–316. [CrossRef]

16. García-Varela, M.; Andrade-Gómez, L. First steps to understand the systematics of Echinorhynchidae Cobbold, 1876 (Acanthocephala), inferred through nuclear gene sequences. *Parasitol. Int.* **2021**, *81*, 102264. [CrossRef]

17. García-Varela, M.; Park, J.-K.; Hernández-Orts, J.S.; Pinacho-Pinacho, C.D. Morphological and molecular data on a new species of *Plagiorhynchus* Lühe, 1911 (Acanthocephala: Plagiorhynchidae) from the long-billed curlew (*Numenius americanus*) from northern Mexico. *J. Helminthol.* **2019**, *94*, e61. [CrossRef]

18. Gazi, M.; Kim, J.; Park, J.-K. The complete mitochondrial genome sequence of *Southwellina hispida* supports monophyly of Palaeacanthocephala (Acanthocephala: Polymorphida). *Parasitol. Int.* **2015**, *64*, 64–68. [CrossRef]

19. Gazi, M.; Kim, J.; García-Varela, M.; Park, C.; Littlewood, D.T.J.; Park, J.-K. Mitogenomic phylogeny of Acanthocephala reveals novel class relationships. *Zool. Scr.* **2016**, *45*, 437–454. [CrossRef]

20. Weber, M.; Wey-Fabrizius, A.R.; Podsiadlowski, L.; Witek, A.; Schill, R.O.; Sugár, L.; Herlyn, H.; Hankeln, T. Phylogenetic analyses of endoparasitic Acanthocephala based on mitochondrial genomes suggest secondary loss of sensory organs. *Mol. Phylogenet. Evol.* **2013**, *66*, 182–189. [CrossRef]

21. Song, F.; Li, H.; Liu, G.-H.; Wang, W.; James, P.; Colwell, D.D.; Tran, A.; Gong, S.; Cai, W.; Shao, R. Mitochondrial genome fragmentation unites the parasitic lice of eutherian mammals. *Syst. Biol.* **2019**, *68*, 430–440. [CrossRef]

22. Muhammad, N.; Suleman; Ma, J.; Khan, M.S.; Wu, S.-S.; Zhu, X.-Q.; Li, L. Characterization of the complete mitochondrial genome of *Centrorhynchus milvus* (Acanthocephala: Polymorphida) and its phylogenetic implications. *Infect. Genet. Evol.* **2019**, *75*, 103946. [CrossRef]

23. Muhammad, N.; Suleman; Ma, J.; Khan, M.S.; Li, L.; Zhao, Q.; Ahmad, M.S.; Zhu, X.-Q. Characterization of the complete mitochondrial genome of *Sphaerirostris picae* (Rudolphi, 1819) (Acanthocephala: Centrorhynchidae), representative of the genus *Sphaerirostris*. *Parasitol. Res.* **2019**, *118*, 2213–2221. [CrossRef]

24. Muhammad, N.; Li, L.; Suleman; Zhao, Q.; Bannai, M.A.; Mohammad, E.T.; Khan, M.S.; Zhu, X.-Q.; Ma, J. Characterization of the complete mitochondrial genome of *Cavisoma magnum* (Acanthocephala: Palaeacanthocephala), first representative of the family Cavisomidae, and its phylogenetic implications. *Infect. Genet. Evol.* **2020**, *80*, 104173. [CrossRef] [PubMed]

25. Muhammad, N.; Suleman; Ahmad, M.S.; Li, L.; Zhao, Q.; Ullah, H.; Zhu, X.-Q.; Ma, J. Mitochondrial DNA dataset suggest that the genus *Sphaerirostris* Golvan, 1956 is a synonym of the genus *Centrorhynchus* Lühe, 1911. *Parasitology* **2020**, *147*, 1149–1157. [CrossRef] [PubMed]

26. Smales, L.R.; Allain, S.J.R.; Wilkinson, J.W.; Harris, E. A new species of *Pseudoacanthocephalus* (Acanthocephala: Echinorhynchidae) from the guttural toad, *Sclerophrys gutturalis* (Bufonidae), introduced into Mauritius, with comments on the implications of the introductions of toads and their parasites into the UK. *J. Helminthol.* **2020**, *94*, e119. [CrossRef] [PubMed]

27. Pichelin, S.; Cribb, T.H. The status of the Diplosentidae (Acanthocephala: Palaeacanthocephala) and a new family of acanthocephalans from Australian wrasses (Pisces: Labridae). *Folia Parasitol. Praha* **2001**, *48*, 289–303. [CrossRef]

28. Braicovich, P.E.; Lanfranchi, A.L.; Farber, M.D.; Marvaldi, A.E.; Luque, J.L.; Timi, J.T. Genetic and morphological evidence reveals the existence of a new family, genus and species of Echinorhynchida (Acanthocephala). *Folia Parasitol. Praha* **2014**, *61*, 377–384. [CrossRef]

29. Monks, S. Phylogeny of the Acanthocephala based on morphological characters. *Syst. Parasitol.* **2001**, *48*, 81–115. [CrossRef]

30. García-Varela, M.; Pérez-Ponce de León, G. Validating the systematic position of *Profilicollis* Meyer, 1931 and *Hexaglandula* Petrochenko, 1950 (Acanthocephala: Polymorphidae) using cytochrome c oxidase (Cox 1). *J. Parasitol.* **2008**, *94*, 212–217. [CrossRef]

31. Petrochenko, V.I. Thorny-headed worms (Acanthocephala) of U. S. S. R. amphibians. In *Contributions on Helminthology in Commemoration of the Birthday of K. I. Skrjabin*; Petrov, A.M., Ed.; Izdatel'stvo Akademii Nauk SSSR: Moscow, Russia, 1953; pp. 507–517.

32. Kennedy, C.R.; Murray, J. A redescription of *Acanthocephalus bufonis* (Shipley, 1903) Southwell and Macfie, 1925 (Acanthocephala: Echinorhynchidae) from the black-spotted toad, *Bufo melanostictus*, from Bogor, Indonesia. *Can. J. Zool.* **1982**, *60*, 356–360. [CrossRef]

33. Wang, Y.-Y. Studies on the life history of *Pseudoacanthpcephalus bufonis* (Shipley, 1903) Petrotschenko, 1958. *J. Fujian Norm. Univ. Nat. Sci. Ed.* **1989**, *5*, 88–93.

34. Bush, S.E.; Duszynski, D.W.; Nickol, B.B. Acanthocephala from Amphibians in China with the description of a new species of *Pseudoacanthocephalus* (Echinorhynchida). *J. Parasitol.* **2009**, *95*, 1440–1445. [CrossRef]

35. Shipley, A.E. On the ento-parasites collected by the "Skeat-Expedition" to Lower Siam and the Malay Peninsula in the years 1899–1900. *Proc. Zool. Soc. Lond.* **1903**, *2*, 145–156.

36. Yuen, P.H.; Fernando, C.H. On *Acanthocephalus bufonis* (Shipley) a Common Parasite of Malayan amphibians. *Bull. natn. Mus. Singap.* **1967**, *33*, 91–93.

37. Herlyn, H.; Röhrig, H. Ultrastructure and overall organization of ligament sac, uterine bell, uterus and vagina in *Paratenuisentis ambiguus* (Acanthocephala, Eoacanthocephala)—The character evolution within the Acanthocephala. *Acta Zool. Stockholm* **2003**, *84*, 239–247. [CrossRef]

38. Zhao, T.-Y.; Zhang, C.-J.; Lv, L. Comparative description of the mitochondrial genome of *Scaphidium formosanum* Pic, 1915 (Coleoptera: Staphylinidae: Scaphidiinae). *Zootaxa* **2021**, *4941*, 487–510. [CrossRef]

39. Jin, J.-J.; Yu, W.-B.; Yang, J.-B.; Song, Y.; de Pamphilis, C.W.; Yi, T.-S.; Li, D.-Z. GetOrganelle: A fast and versatile toolkit for accurate de novo assembly of organelle genomes. *Genome Biol.* **2020**, *21*, 241. [CrossRef]

40. Meng, G.; Li, Y.; Yang, C.; Liu, S. MitoZ: A toolkit for animal mitochondrial genome assembly, annotation and visualization. *Nucleic Acids Res.* **2019**, *47*, e63. [CrossRef]

41. Gruber, A.R.; Bernhart, S.H.; Lorenz, R. The ViennaRNA Web Services. In *RNA Bioinformatics*; Picardi, E., Ed.; Methods in Molecular Biology; Springer: New York, NY, USA, 2015; Volume 1269, pp. 307–326. ISBN 978-1-4939-2291-8.

42. Bernt, M.; Merkle, D.; Ramsch, K.; Fritzsch, G.; Perseke, M.; Bernhard, D.; Schlegel, M.; Stadler, P.F.; Middendorf, M. CREx: Inferring genomic rearrangements based on common intervals. *Bioinformatics* **2007**, *23*, 2957–2958. [CrossRef]

43. Reuter, J.S.; Mathews, D.H. RNAstructure: Software for RNA secondary structure prediction and analysis. *BMC Bioinform.* **2010**, *11*, 129. [CrossRef]

44. Lee, B.D. Python implementation of codon adaptation index. *J. Open Source Softw.* **2018**, *3*, 905. [CrossRef]

45. Katoh, K.; Standley, D.M. MAFFT multiple sequence alignment software version 7: Improvements in performance and usability. *Mol. Biol. Evol.* **2013**, *30*, 772–780. [CrossRef]

46. Criscuolo, A.; Gribaldo, S. BMGE (Block Mapping and Gathering with Entropy): A new software for selection of phylogenetic informative regions from multiple sequence alignments. *BMC Evol. Biol.* **2010**, *10*, 210. [CrossRef] [PubMed]

47. Zhang, D.; Gao, F.; Jakovlić, I.; Zou, H.; Zhang, J.; Li, W.X.; Wang, G.T. PhyloSuite: An integrated and scalable desktop platform for streamlined molecular sequence data management and evolutionary phylogenetics studies. *Mol. Ecol. Resour.* **2020**, *20*, 348–355. [CrossRef] [PubMed]

48. Lartillot, N.; Rodrigue, N.; Stubbs, D.; Richer, J. PhyloBayes MPI: Phylogenetic reconstruction with infinite mixtures of profiles in a parallel environment. *Syst. Biol.* **2013**, *62*, 611–615. [CrossRef] [PubMed]

49. Lartillot, N.; Philippe, H. A bayesian mixture model for across-site heterogeneities in the amino-acid replacement process. *Mol. Biol. Evol.* **2004**, *21*, 1095–1109. [CrossRef]

50. Lartillot, N.; Philippe, H. Computing bayes factors using thermodynamic integration. *Syst. Biol.* **2006**, *55*, 195–207. [CrossRef]

51. Lartillot, N.; Brinkmann, H.; Philippe, H. Suppression of long-branch attraction artefacts in the animal phylogeny using a site-heterogeneous model. *BMC Evol. Biol.* **2007**, *7*, S4. [CrossRef]

52. Minh, B.Q.; Schmidt, H.A.; Chernomor, O.; Schrempf, D.; Woodhams, M.D.; von Haeseler, A.; Lanfear, R. IQ-TREE 2: New models and efficient methods for phylogenetic inference in the genomic era. *Mol. Biol. Evol.* **2020**, *37*, 1530–1534. [CrossRef]

53. Kalyaanamoorthy, S.; Minh, B.Q.; Wong, T.K.F.; von Haeseler, A.; Jermiin, L.S. ModelFinder: Fast model selection for accurate phylogenetic estimates. *Nat. Methods* **2017**, *14*, 587–589. [CrossRef]

54. Le, S.-Q.; Gascuel, O.; Lartillot, N. Empirical profile mixture models for phylogenetic reconstruction. *Bioinformatics* **2008**, *24*, 2317–2323. [CrossRef]

55. Golombek, A.; Tobergte, S.; Struck, T.H. Elucidating the phylogenetic position of Gnathostomulida and first mitochondrial genomes of Gnathostomulida, Gastrotricha and Polycladida (Platyhelminthes). *Mol. Phylogenet. Evol.* **2015**, *86*, 49–63. [CrossRef]

56. Chernomor, O.; von Haeseler, A.; Minh, B.Q. Terrace aware data structure for phylogenomic inference from supermatrices. *Syst. Biol.* **2016**, *65*, 997–1008. [CrossRef]

57. Letunic, I.; Bork, P. Interactive tree of life (iTOL) v5: An online tool for phylogenetic tree display and annotation. *Nucleic Acids Res.* **2021**, *49*, W293–W296. [CrossRef]

58. Steinauer, M.L.; Nickol, B.B.; Broughton, R.; Ortí, G. First sequenced mitochondrial genome from the phylum Acanthocephala (*Leptorhynchoides thecatus*) and its phylogenetic position within Metazoa. *J. Mol. Evol.* **2005**, *60*, 706–715. [CrossRef]

59. Pan, T.S.; Nie, P. The complete mitochondrial genome of *Pallisentis celatus* (Acanthocephala) with phylogenetic analysis of Acanthocephalans and Rotifers. *Folia Parasitol.* **2013**, *60*, 181–191. [CrossRef]
60. Song, R.; Zhang, D.; Deng, S.; Ding, D.; Liao, F.; Liu, L. The complete mitochondrial genome of *Acanthosentis cheni* (Acanthocephala: Quadrigyridae). *Mitochondrial DNA Part B* **2016**, *1*, 797–798. [CrossRef]
61. Pan, T.; Jiang, H. The complete mitochondrial genome of *Hebesoma Violentum* (Acanthocephala). *Mitochondrial DNA Part B* **2018**, *3*, 582–583. [CrossRef]
62. Lei, M.-T.; Cai, J.-Z.; Li, C.-H.; Fu, Y.; Sun, J.; Ma, D.-D.; Li, Y.-P.; Zhang, Y.-M. Prevalence and genetic diversity of *Echinorhynchus gymnocyprii* (Acanthocephala: Echinorhynchidae) in schizothoracine fishes (Cyprinidae: Schizothoracinae) in Qinghai-Tibetan Plateau, China. *Parasite. Vector* **2020**, *13*, 357. [CrossRef]
63. Mauer, K.; Hellmann, S.L.; Groth, M.; Fröbius, A.C.; Zischler, H.; Hankeln, T.; Herlyn, H. The genome, transcriptome, and proteome of the fish parasite *Pomphorhynchus laevis* (Acanthocephala). *PLoS ONE* **2020**, *15*, e0232973. [CrossRef]
64. Muhammad, N.; Suleman; Khan, M.S.; Li, L.; Zhao, Q.; Ullah, H.; Zhu, X.-Q.; Ma, J. Characterization of the complete mitogenome of *Centrorhynchus clitorideus* (Meyer, 1931) (Palaeacanthocephala: Centrorhynchidae), the largest mitochondrial genome in Acanthocephala, and its phylogenetic implications. *Mol. Biochem. Parasitol.* **2020**, *237*, 111274. [CrossRef]
65. Kilpert, F.; Podsiadlowski, L. The complete mitochondrial genome of the common sea slater, *Ligia oceanica* (Crustacea, Isopoda) bears a novel gene order and unusual control region features. *BMC Genomics* **2006**, *7*, 241. [CrossRef]
66. Song, R.; Zhang, D.; Gao, J.-W.; Cheng, X.-F.; Xie, M.; Li, H.; Wu, Y.-A. Characterization of the complete mitochondrial genome of *Brentisentisyangtzensis* Yu & Wu, 1989 (*Acanthocephala, Illiosentidae*). *ZooKeys* **2019**, *861*, 1–14. [CrossRef] [PubMed]
67. Sarwar, H.; Zhao, W.-T.; Kibet, C.J.; Sitko, J.; Nie, P. Morphological and complete mitogenomic characterisation of the Acanthocephalan *Polymorphus minutus* infecting the duck anas platyrhynchos. *Folia Parasitol.* **2021**, *68*, e015. [CrossRef] [PubMed]
68. García-Varela, M.; González-Oliver, A. The systematic position of *Leptorhynchoides* (Kostylew, 1924) and *Pseudoleptorhynchoides* (SalgadoMaldonado, 1976), inferred from nuclear and mitochondrial DNA gene sequences. *J. Parasitol.* **2008**, *94*, 959–962. [CrossRef] [PubMed]
69. García-Varela, M.; Pérez-Ponce de León, G.; Aznar, F.J.; Nadler, S.A. Phylogenetic relationship among genera of Polymorphidae (Acanthocephala), inferred from nuclear and mitochondrial gene sequences. *Mol. Phylogenet. Evol.* **2013**, *68*, 176–184. [CrossRef] [PubMed]
70. Tkach, V.V.; Lisitsyna, O.I.; Crossley, J.L.; Binh, T.T.; Bush, S.E. Morphological and molecular differentiation of two new species of *Pseudoacanthocephalus* Petrochenko, 1958 (Acanthocephala: Echinorhynchidae) from amphibians and reptiles in the Philippines, with identification key for the genus. *Syst. Parasitol.* **2013**, *85*, 11–26. [CrossRef]
71. Herlyn, H.; Piskurek, O.; Schmitz, J.; Ehlers, U.; Zischler, H. The syndermatan phylogeny and the evolution of acanthocephalan endoparasitism as inferred from 18S rDNA sequences. *Mol. Phylogenet. Evol.* **2003**, *26*, 155–164. [CrossRef]
72. Witek, A.; Herlyn, H.; Meyer, A.; Boell, L.; Bucher, G.; Hankeln, T. EST based phylogenomics of Syndermata questions monophyly of Eurotatoria. *BMC Evol. Biol.* **2008**, *8*, 345. [CrossRef]
73. Wey-Fabrizius, A.R.; Herlyn, H.; Rieger, B.; Rosenkranz, D.; Witek, A.; Welch, D.B.M.; Ebersberger, I.; Hankeln, T. Transcriptome data reveal syndermatan relationships and suggest the evolution of endoparasitism in Acanthocephala via an epizoic stage. *PLoS ONE* **2014**, *9*, e88618. [CrossRef]
74. Abdel-Ghaffar, F.; Morsy, K.; Abdel-Gaber, R.; Mehlhorn, H.; Al Quraishy, S.; Mohammed, S. Prevalence, morphology, and molecular analysis of *Serrasentis sagittifer* (Acanthocephala: Palaeacanthocephala: Rhadinorhynchidae), a parasite of the gilthead sea bream *Sparus aurata* (Sparidae). *Parasitol. Res.* **2014**, *113*, 2445–2454. [CrossRef]
75. Costa Fernandes, V.S.; Amin, O.; Borges, J.N.; Santos, C.P. A new species of the Acanthocephalan genus *Filisoma* (Cavisomidae) from perciform fishes in Rio de Janeiro, Brasil. *Acta Parasit.* **2019**, *64*, 176–186. [CrossRef]